A Robust UWB Indoor Positioning System for Highly Complex Environments

Enrique García, Pablo Poudereux, Álvaro Hernández, Jesús Ureña, David Gualda

Department of Electronics, University of Alcalá
Alcalá de Henares (Madrid), Spain
Email: enrique.garcia@depeca.uah.es

***Abstract*—Ultra-Wideband (UWB) has a high interest in research and industry for accurate indoor positioning. This technology comprises signals with a bandwidth of at least 500 MHz at a power decay of -10dB. This large bandwidth conferes the capability of resolving multipath, penetrating through obstacles and accurate ranging. However, NLOS (Non-Line-Of-Sight) conditions produced by obstacles in indoor environments severely degrade performance, as they introduce a positive bias in ranging estimation. In this paper we present a robust UWB indoor positioning which is able to accurately operate in a highly complex indoor scenario, where NLOS condition is predominant. For that purpose, the system uses a NLOS detection algorithm based on the skewness of the estimated channel impulse response and it mitigates NLOS by using an Extended Kalman Filter. The use of this detection/mitigation algorithm shows an improvement of the RMSE in positioning about 67%.**

***Index Terms*—Localization, Ultra-Wideband (UWB), Non-Line-Of-Sight (NLOS), Extended Kalman Filter (EKF).**

I. Introduction

Ultra-wideband indoor positioning systems have been proposed for highly accurate solutions, where other radio-frequency technologies as WiFi, Zigbee or Bluetooth cannot offer those accuracy levels. There are several research works that propose the use of UWB for positioning on industrial wireless sensor networks [1], [2]. Also, there are already some commercially available solutions for industry and the so-called Internet of Things (IoT) [3], [4]. Most of the highly accurate UWB positioning systems available in literature seem to work in very controlled environments [5]–[7]. However, under NLOS (Non-Line-Of-Sight) conditions, which is the common case in complex indoor environments, there is a severe loss in the positioning precision of UWB systems [8], due to the fact that obstacles produces a positive bias in ranging estimation, which depends on the dielectric properties of the obstacle [9].

For that reason, there is a high research interest in NLOS mitigation for UWB indoor positioning. Several works have dealt with those errors for UWB by using algorithms for identifying the NLOS conditions and for mitigating them [10]–[12], although this problem had already been researched before for mobile phone localization [13], [14]. Detection algorithms are mostly based on channel statistics, such as kurtosis, delay spread or a running variance of the estimated Time Of Arrival (TOA); for more information see [15] and references therein. Most of the previous research in NLOS detection/mitigation for UWB use the simulated channel model to validate algorithms; although there are some exceptions that use real data [11], [12], [16].

In this work we improve the positioning accuracy of an UWB indoor positioning system presented in [17] by using an NLOS detection and mitigation algorithm. We propose the use of the skewness of the estimated channel impulse response as a parameter to detect the NLOS condition and an Extended Kalman Filter for accurately positioning in harsh environments. The robustness of the positioning system is verified by means of experimental data.

The rest of this manuscript has been organized as follows: Section II provides a review of the UWB indoor positioning system; Section III describes the signal processing techniques used for TDOA estimation and it presents the NLOS identification and mitigation algorithm, whereas Section IV shows some experimental results of the measurement campaign with the positioning system. Finally in Section V, we derive the conclusions from this work.

II. UWB Platform

The UWB platform proposed in [17] is an asynchronous DS-UWB indoor positioning system developed with Commercial Off-The-Shelf (COTS) components. It is formed by $N = 4$ emitting beacons placed on the ceiling of a highly complex environment and a receiver that works out its position. Fig. 1 shows a block diagram of the UWB indoor positioning system, not only for the emitting beacons but also for the receiver.

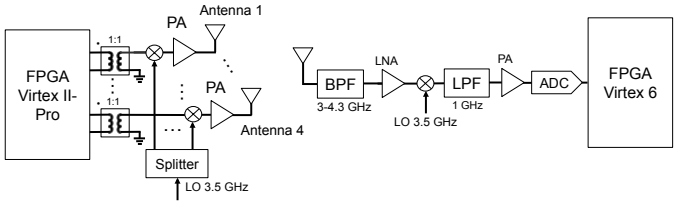

Figure 1. Block diagram of the UWB system, for the emitting beacons (left part) and for the receiver (right part).

The emission is controlled by a Xilinx Virtex II FPGA, which transmits simultaneously four Loosely Synchronized (LS) spreading sequences [18] of length $L = 1039$ bits at a

978-1-4799-7800-7/15/$31.00 ©2015 IEEE

bitrate of 500 Mbps. The baseband signals are then multiplied by a 3.5 GHz carrier wave, which directly translates the transmitted signals to that central frequency with a bandwidth of 577 MHz at a power decay of -10 dB. Each of these signals is passed through a bank of Power Amplifiers (PA) and emitted simultaneously and periodically.

The received signal is passed through a Band-Pass Filter (BPF) to amplify only the frequencies of interest. Then it is directly down-converted to baseband by using a 3.5 GHz local oscillator. This baseband signal is again filtered with a Low-Pass Filter and amplified to adjust the signal levels to the ADC span. The receiver is controlled by a Xilinx FPGA Virtex 6 that processes the acquired samples from a 10-bit resolution ADC with a sampling rate of 5GS/s. As stated previously, the UWB positioning system is asynchronous, so the receiver does not have information about the transmission time from the beacons; for that reason the receiver must acquire a frame long enough to ensure that it contains the transmitted signal from each beacon. In contrast to a majority of the UWB positioning systems presented in literature, which use TDMA to avoid multiple access interferences and near-far effect, this platform uses a CDMA scheme, thus reducing the input buffer size required to ensure the acquisition of a complete frame.

After acquiring the frame, the receiver computes the Time Differences Of Arrival (TDOAs) between the receiver and each beacon and it applies a Gauss-Newton hyperbolic positioning algorithm [19]. For more implementation details, refer to [17].

Fig. 2 depicts the scenario where the UWB platform is deployed. It is a dynamic and complex environment, where people, furniture and different objects obstructs the arriving signals from most of the beacons.

Figure 2. Environment in which the UWB positioning system is deployed.

Under this complex conditions, the UWB platform described in [17] has a poor performance. Here we will provide robustness to this UWB indoor positioning system to work precisely under harsh environments by deriving an NLOS detection/mitigation algorithm.

III. Signal Processing

As has been previously commented, the UWB platform uses CDMA instead of TDMA. The main challenges of CDMA is near-far effect and Multiple-Access Interferences (MAI), which typically are dealt by using bulky power control systems [20] and complex interference mitigation algorithms like Successive Interference Cancellation (SIC) [21]. On the contrary, the UWB platform shown here deals with near-far effect and MAI in an efficient form by using LS codes.

Given two ternary and unitary codes of length L, $\{s_u[l], s_v[l]\}; 0 \leq l \leq L-1$, they are LS codes if their discrete aperiodic correlation function, $C_{s_u,s_v}[\tau]$, is as follows (1):

$$C_{s_u,s_v}[\tau] = \sum_{l=0}^{L-1-\tau} s_u[l] \cdot s_v[l+\tau] = \begin{cases} E, \text{ for } \tau = 0 & u = v \\ 0, \text{ for } 1 \leq |\tau| \leq W & u = v \\ 0, \text{ for } 0 \leq |\tau| \leq W & u \neq v \end{cases} \quad (1)$$

where W is the Zero Correlation Zone (ZCZ), which allows to jointly estimate the channel impulse response and effectively mitigate MAI. To ensure that all the correlation peaks are within the ZCZ (thus avoiding near-far and MAI) the maximum feasible TDOA for a given coverage area should be lower than the ZCZ size. Here we have use LS codes with length $L = 1039$ bits which have a ZCZ length large enough to meet the previous restriction.

In order to estimate the first arriving path, the receiver follows the steps depicted in Fig. 3. At each position, the receiver performs the correlation of the received signal with the four transmitted signals; later the absolute value of each correlation signal is carried out and the receiver uses a window of 201 samples around the overall maximum correlation peak to estimate the time of arrival for each transmitted signal. Fig. 4 shows the absolute value of the aperiodic correlations between the received signal and each of the transmitted signal as well as the window applied for searching the first arriving path for every link.

Inside this window, the algorithm searches back the first sample that exceeds a given threshold. In this system it has been considered the 40% of the maximum correlation value for each beacon.

A. NLOS Detection

After the TDOAs are computed, the algorithm estimates the LOS/NLOS condition for each of the transmission link. We propose the use of the skewness of the channel estimation for that purpose as it is a natural form of determining the mass of the channel impulse response, which can be efficiently estimated thanks to the ideal aperiodic correlation function of LS codes within the ZCZ and the existence of fast correlators [22].

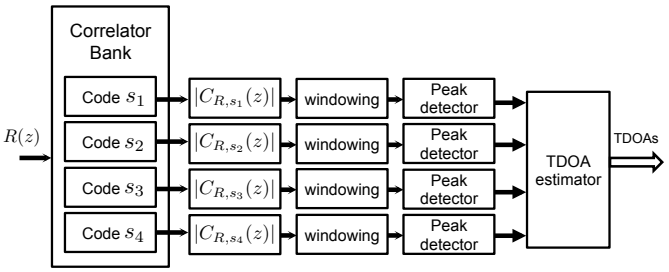

Figure 3. Block diagram of the signal processing carried out for TDOA estimation.

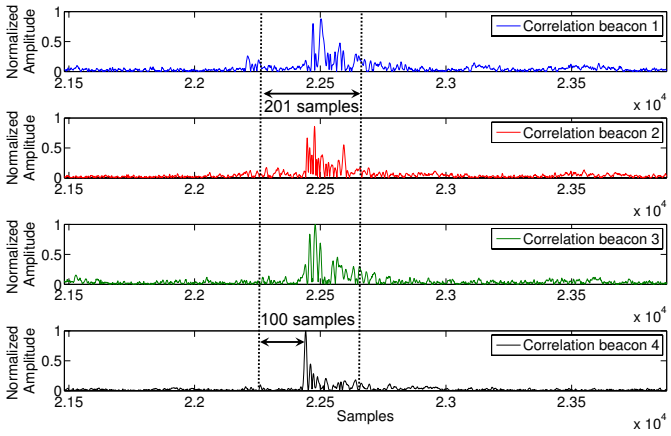

Figure 4. Aperiodic correlations between received signal and each transmitted signal.

The skewness of a probability density function (pdf) is a measurement of its asymmetry around its mean. It is defined as (2):

$$\gamma = \frac{\mathrm{E}[(\mathcal{C}[\tau] - \mu)^3]}{(\mathrm{E}[\mathcal{C}[\tau] - \mu)]^2)^{3/2}} \tag{2}$$

where $\mathcal{C}[\tau]$ is the aperiodic correlation function defined in (1) inside a window $\mathcal{W}$. A negative skewness refers to an asymmetry in the pdf to the left whereas a positive skewness refers to an asymmetry to the right. For that reason, it is expected a lower skewness in NLOS than in LOS condition. Fig. 5 shows the absolute value of the correlation function for a window $\mathcal{W} = 201$ samples and centered around the maximum correlation peak. As expected, the LOS condition has a larger skewness (i.e. its mass is more concentrated to the right side).

Considering this parameter, we can classify the LOS/NLOS condition by using a likelihood ratio test, equal to [10]:

$$Classify: \begin{cases} LOS: & if\ \frac{P(\gamma/LOS)}{P(\gamma/NLOS)} \geq \frac{P(NLOS)}{P(LOS)} \\ NLOS: & if\ \frac{P(\gamma/LOS)}{P(\gamma/NLOS)} < \frac{P(NLOS)}{P(LOS)} \end{cases} \tag{3}$$

Assuming that $P(NLOS) = P(LOS)$ the binary classifier can be expressed as [11]:

$$Classify: \begin{cases} LOS: & \gamma \geq \lambda \\ NLOS: & \gamma < \lambda \end{cases} \tag{4}$$

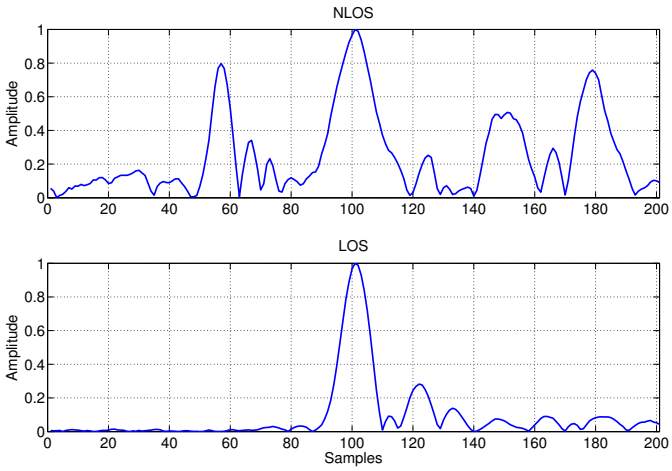

Figure 5. Correlation functions in NLOS and LOS conditions.

where the threshold λ is the intersection between the conditional pdfs, i.e. the value at $P(\gamma/LOS) = P(\gamma/NLOS)$.

Several works use a similar approach by using a joint likelihood ratio test and considering parameters such as delay spread, energy of the received signal, kurtosis of the channel impulse response, assuming they are independent random variables [10], [11]. Here we will show that the use of the skewness is a sufficient parameter to significantly improve the system performance.

In order to determine the skewness of each correlation function, it is chosen a window of $\mathcal{W} = 201$ samples within the IFW and around the maximum correlation peak of each correlation. Then the classifier in equation (4) is applied to every windowed correlation function. If the link between the receiver and the reference beacon is obstructed, the error will affect the computation of all the TDOAs. For this reason, if that link is classified as NLOS, the three resulting TDOAs (number of beacons, $N = 4$) are considered as affected by NLOS, regardless the condition of the other links. On the other hand, if the link between the receiver and the reference beacon is classified as LOS, the TDOA state will depend on the particular link condition.

B. NLOS Mitigation

After the NLOS condition has been detected for every TDOAs measurement, they are used along with an Extended Kalman Filter (EKF) to determine the position of the receiver. In this work we have used the EKF as a smoother of the NLOS errors; hence we do not use the prediction stage of the EKF, as the mobile does not change its position during the computation of its location. The update stage are defined as [23]:

$$\begin{aligned} \mathbf{K}_k &= \mathbf{P}_k^- \cdot \mathbf{H}_k^T \cdot [\mathbf{H}_k \cdot \mathbf{P}_k^- \cdot \mathbf{H}_k^T + \mathbf{R}_k]^{-1} \\ \hat{\mathbf{x}}_k &= \hat{\mathbf{x}}_k^- + \mathbf{K}_k \cdot (\mathbf{z}_k - \mathbf{h}(\hat{\mathbf{x}}_k^-)) \\ \mathbf{P}_k &= (\mathbf{I} - \mathbf{K}_k \cdot \mathbf{H}_k) \cdot \mathbf{P}_k^- \end{aligned} \tag{5}$$

where $\mathbf{K}_k$ is the Kalman gain at time instant k; $\mathbf{P}_k^-$ is the a priori covariance matrix at time instant k; $\mathbf{z}_k$ is the TDOA measured vector at k; and $\hat{\mathbf{x}}_k = [\hat{x}_k, \hat{y}_k]^T$is the state vector which is equal to the 2D position of the mobile at k. The observation noise matrix, $\mathbf{R}_k$, is defined as

$$\mathbf{R}_k = \begin{bmatrix} \sigma_{1,k}^2 + \sigma_{2,k}^2 & \sigma_{1,k}^2 & \sigma_{1,k}^2 \\ \sigma_{1,k}^2 & \ddots & \sigma_{1,k}^2 \\ \sigma_{1,k}^2 & \sigma_{1,k}^2 & \sigma_{1,k}^2 + \sigma_{N,k}^2 \end{bmatrix} \quad (6)$$

and the entry values $\{\sigma_{1,k}^2, \ldots, \sigma_{N,k}^2\}$ depend on the NLOS condition measured for each link as we show later.

The vector $\mathbf{h}(\hat{\mathbf{x}}_k^-)$ is defined as

$$\mathbf{h}(\hat{\mathbf{x}}_k^-) = \begin{bmatrix} h_1(\hat{\mathbf{x}}_k^-) \\ \vdots \\ h_{N-1}(\hat{\mathbf{x}}_k^-) \end{bmatrix} \quad (7)$$

where $h_i(\hat{\mathbf{x}}_k^-)$, $1 \leq i \leq N-1$ is the a priori estimated TDOA and equal to [24]:

$$h_i(\hat{\mathbf{x}}_k^-) = \sqrt{(\hat{x}_k^- - \alpha_{i+1})^2 + (\hat{y}_k^- - \beta_{i+1})^2 + (z_M - \gamma_{i+1})^2} - \sqrt{(\hat{x}_k^- - \alpha_1)^2 + (\hat{y}_k^- - \beta_1)^2 + (z_M - \gamma_1)^2} \quad (8)$$

where z_M is the receiver height and $(\alpha_n, \beta_n, \gamma_n)$ are the cartesian coordinates of the beacon $n, 1 \leq n \leq N$.

The observation matrix $\mathbf{H}_k$ is defined as the following Jacobian:

$$\mathbf{H}_k = \begin{bmatrix} \frac{\partial h_1(\hat{\mathbf{x}}_k^-)}{\partial \hat{x}_k^-} & \frac{\partial h_1(\hat{\mathbf{x}}_k^-)}{\partial \hat{y}_k^-} \\ \vdots & \vdots \\ \frac{\partial h_{N-1}(\hat{\mathbf{x}}_k^-)}{\partial \hat{x}_k^-} & \frac{\partial h_{N-1}(\hat{\mathbf{x}}_k^-)}{\partial \hat{y}_k^-} \end{bmatrix} \quad (9)$$

where the partial derivatives are defined as depicted in equations (10) and (11).

The a priori covariance matrix $\mathbf{P}_k^-$ is initialized at $k = 0$ as $\mathbf{P}_0^- = 20 \cdot \mathbf{I}$ in meters and the initial state vector $\hat{\mathbf{x}}_0$ is obtained from a Gauss-Newton hyperbolic positioning algorithm. For each time instant k, if the identification stage detects a TOA measurement affected by NLOS, the variance $\sigma_{i,k}^2$ of the noise matrix $\mathbf{R}_k$ is set to 3 meters whereas in any other case it is set to 0.5 meters. In this way, the EKF reduces the confidence on TDOAs measurements affected by NLOS and it minimizes the variance of the positioning errors.

IV. Results

For the following results, the receiver has computed 100 ranging measurements from each beacon for 48 different positions within the coverage area. Table I shows the coordinates of the beacons in metres.

In order to determine the trueness of the positioning system, the ground truth is determined by using the junctions of the 40×40 cm floor tiles. The UWB antenna has been placed at a height of 1.57 m, which is lower than the height of the furnitures in the room. Also the FPGA of the receiver has been replaced by a 5GS/s digital sampling oscilloscope to evaluate the goodness of the proposed mitigation algorithm and future improvements under the same channel conditions. Therefore, the NLOS detection/mitigation algorithm has been run in a laptop with MATLAB. Fig. 6 depicts the projections on the floor of the 48 test positions and the four beacons as well as the distribution of the furnitures in the room.

Table I
POSITIONS IN METRES OF THE BEACONS IN THE EXPERIMENTAL SETUP.

Beacon (n)	α_n	β_n	γ_n
1	-0.281	4.19	2.80
2	-0.226	-1.39	2.80
3	7.14	-1.38	2.81
4	5.84	2.09	2.82

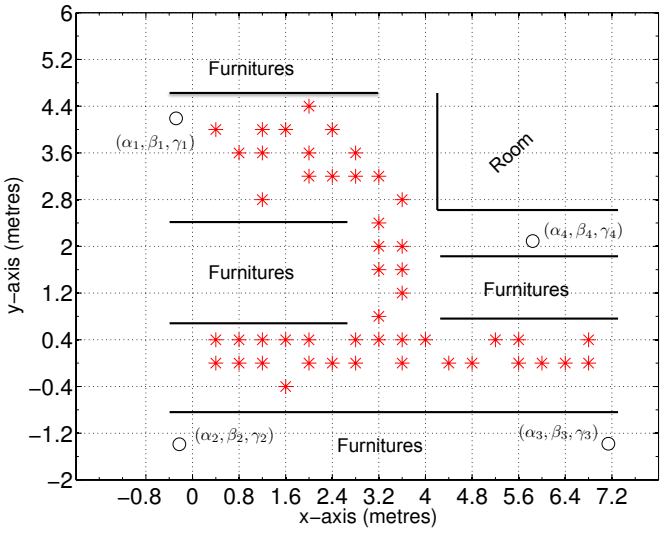

Figure 6. Projection of the 48 test positions and the beacons on the floor.

The threshold λ, used for NLOS detection of each link, has been experimentally determined at $\lambda = 1.99$. Table II shows the global RMSE (Root Mean Squared Error) in metres for each axis among the 48 test positions when no NLOS detection/mitigation algorithm is applied and with the explained algorithm. It shows an average improvement in the RMSE about 67% compared to the one obtained without NLOS mitigation.

Table II
GLOBAL RMSE IN POSITIONING FOR EACH AXIS CONSIDERING 48 TEST POSITIONS.

	RMSE $\hat{x}$	RMSE $\hat{y}$
No mitigation	1.42	0.85
EKF	0.43	0.38

In order to show the robustness of the DS-UWB system to near-far effect and NLOS, below we depict the positioning results in two test positions close to a given beacon with

$$\frac{\partial h_i(\hat{\mathbf{x}}_k^-)}{\partial \hat{x}_k^-} = \frac{\hat{x}_k^- - \alpha_{i+1}}{\sqrt{(\hat{x}_k^- - \alpha_{i+1})^2 + (\hat{y}_k^- - \beta_{i+1})^2 + (z_M - \gamma_{i+1})^2}} - \frac{\hat{x}_k^- - \alpha_1}{\sqrt{(\hat{x}_k^- - \alpha_1)^2 + (\hat{y}_k^- - \beta_1)^2 + (z_M - \gamma_1)^2}} \quad (10)$$

$$\frac{\partial h_1(\hat{\mathbf{x}}_k^-)}{\partial \hat{y}_k^-} = \frac{\hat{y}_k^- - \beta_{i+1}}{\sqrt{(\hat{x}_k^- - \alpha_{i+1})^2 + (\hat{y}_k^- - \beta_{i+1})^2 + (z_M - \gamma_{i+1})^2}} - \frac{\hat{y}_k^- - \beta_1}{\sqrt{(\hat{x}_k^- - \alpha_1)^2 + (\hat{y}_k^- - \beta_1)^2 + (z_M - \gamma_1)^2}} \quad (11)$$

coordinates $(0.4, 0, 1.57)$ and $(1.20, 2.80, 1.57)$. Fig. 7 depicts the Cumulative Distribution Function (CDF) of the mean absolute error in positioning in metres for each axis for the coordinates $(0.4, 0, 1.57)$.

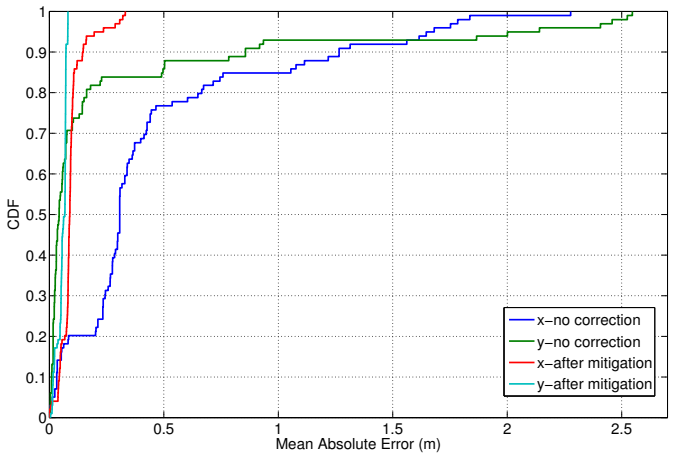

Figure 7. CDF of the positioning error (x, y) in the coordinates $(0.4, 0, 1.57)$ before and after mitigation.

On the other hand, Fig. 8 shows the 100 positioning estimations without any NLOS correction (i.e. the results obtained with a hyperbolic Gauss-Newton algorithm) and the estimations when using the NLOS mitigation algorithm in the position $(1.20, 2.80, 1.57)$. It can be observed how this algorithm greatly improves the trueness of the positioning system, achieving RMSE values for this position equal to 41 cm in the x-axis and 22 cm in the y-axis.

V. Conclusions

UWB promises high accuracy for indoor positioning systems. Nonetheless, in practice this occurs under very controlled environments, where LOS condition predominates. In a more realistic scenario, UWB indoor positioning systems are severely degraded by a bias in ranging estimation caused by objects. In this paper we have shown a DS-UWB indoor positioning system deployed in a realistic scenario, where transmitted signals are obstructed by moving people, furnitures and a range of different objects. Under these conditions, the systems have a large RMSE in positioning. To deal with these NLOS errors, we have proposed the use of a NLOS identification and mitigation algorithm. For NLOS identification, we have used the skewness of the estimated channel impulse response, which can be efficiently estimated thanks to the use of LS codes. Furthermore, NLOS mitigation has been achieved by modifying the noise matrix of an EKF according to the identification results for each link. The results of this algorithm show an improvement of the trueness in positioning approximately in a 67%.

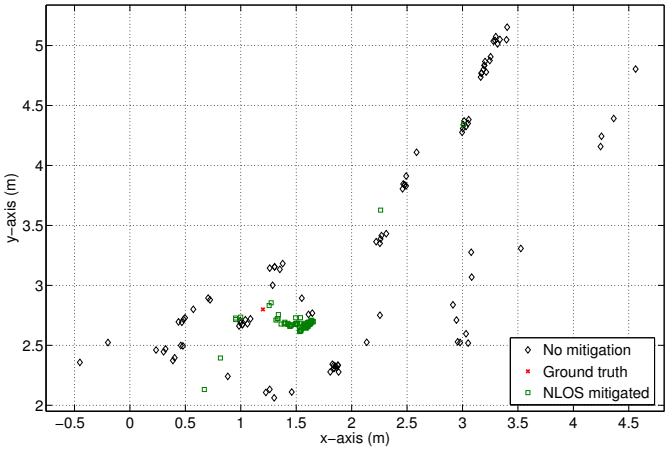

Figure 8. Positioning results for the coordinates $(1.20, 2.8, 1.57)$ before and after NLOS mitigation.

VI. Acknowledgements

This work was supported by the Spanish Ministry of Economy and Competitiveness (LORIS Project, ref. TIN2012-38080-C04-01, DISSECT-SOC Project, ref. TEC2012-38058-C03-03) and by the University of Alcalá (CODECSS Project, ref. CCG2013/EXP-080).

References

[1] G. P. Hancke and B. Allen, "Ultrawideband as an Industrial Wireless Solution," *IEEE Pervasive Computing*, vol. 5, no. 4, pp. 78–85, 2006.
[2] L. Zwirello, M. Janson, and T. Zwick, "Ultra-wideband based positioning system for applications in industrial environments," in *Proceedings of 2010 European Wireless Technology Conference*, 2010, pp. 165–168.
[3] ubisense, http://www.ubisense.net, 2014.
[4] DecaWave, http://www.decawave.com, 2014.
[5] O. Cetin, H. Nazli, R. Gurcan, H. Ozturk, H. Guneren, Y. Yelkovan, M. Cayir, H. Celebi, and H. P. Partal, "An experimental study of high precision TOA based UWB positioning systems," in *Proceedings of the IEEE International Conference on Ultra-Wideband (ICUWB)*, 2012, pp. 357–361.
[6] M. M. Pietrzyk and T. von der Grün, "Experimental validation of a TOA UWB ranging platform with the energy detection receiver," in *Proceedings of the International Conference on Indoor Positioning and Indoor Navigation*, 2010, pp. 1–8.
[7] Z. N. Low, J. H. Cheong, C. L. Law, W. T. Ng, and Y. J. Lee, "Pulse detection algorithm for Line-Of-Sight (LOS) UWB ranging applications," *IEEE Antennas and Wireless Propagation Letters*, vol. 4, pp. 63–67, 2005.

[8] F. Zampella, A. R. Jiménez, and F. Seco, "Robust indoor positioning fusing PDR and RF technologies: The RFID and UWB case," in *Proceedings of 2013 International Conference on Indoor Positioning and Indoor Navigation*, 2013, pp. 1–7.

[9] A. Muqaibel, A. Safaai-Jazi, A. Bayram, and A. M. Attiya, "Ultrawideband through-the-wall propagation," *IEE Proceedings- Microwaves, Antennas and Propagation*, pp. 581–588, 2005.

[10] I. Guvenc, C.-C. Chong, and F. Watanabe, "NLOS identification and mitigation for UWB localization system," in *Proceedings of the 2007 IEEE Wireless Communications and Networking Conference*, 2007, pp. 1571–1576.

[11] N. Decarli, D. Dardari, S. Gezici, and A. A. D'Amico, "LOS/NLOS detection for UWB signals: A comparative study using experimental data," in *Proceedings of the 5th IEEE International Symposium on Wireless Pervasive Computing*, 2010, pp. 169–173.

[12] J. Schroeder, S. Galler, K. Kyamakya, and T. Kaiser, "Three-dimensional indoor localization in Non Line of Sight UWB channels," in *Proceedings of the 2007 IEEE International Conference on Ultra-Wideband*, 2007, pp. 89–93.

[13] M. P. Wylie and J. Holtzman, "The Non-Line of Sight problem in mobile location estimation," in *Proceedings of the IEEE International Conference on Universal Personal Communications*, vol. 2, 1996, pp. 827–831.

[14] P.-C. Chen, "A non-line-of-sight error mitigation algorithm in location estimation," in *Proceedings of IEEE Wireless Communications and Networking Conference*, vol. 1, 1999, pp. 316–320.

[15] J. Khodjaev, Y. Park, and A. S. Malik, "Survey of NLOS identification and error mitigation problems in UWB-based positioning algorithms for dense environments," *Annals of Telecommunications*, vol. 65, no. 5-6, pp. 301–311, 2010.

[16] S. Marano, W. M. Gifford, H. Wymeersch, and M. Z. Win, "NLOS identification and mitigation for localization based on UWB experimental data," *IEEE Journal on Selected Areas in Communications*, vol. 28, no. 7, pp. 1026–1035, 2010.

[17] E. García, P. Poudereux, A. Hernández, J. J. García, and J. Ureña, "DS-UWB indoor positioning system implementation based on FPGAs," *Sens. Actuators, A*, vol. 201, pp. 172–181, 2013.

[18] S. Stanczak, H. Boche, and M. Haardt, "Are LAS-codes a miracle?" in *Proceedings of the 2001 IEEE Global Telecommunications Conference, GLOBECOM '01*, vol. 1, 2001, pp. 589–593.

[19] N. Sirola, "Close-form algorithms in mobile positioning: myths and misconceptions," in *Proceedings of the 7th Workshop in Positioning Navigation and Communication (WPNC'10)*, 2010, pp. 38–44.

[20] W.-M. Tam and F. C. M. Lau, "Analysis of power control and its imperfections in CDMA cellular systems," *IEEE Transactions on Vehicular Technology*, vol. 48, no. 5, pp. 1706–1717, 1999.

[21] J. M. Holtzman, "DS/CDMA successive interference cancellation," in *Proceedings of the IEEE 3rd International Symposium on Spread Spectrum Techniques and Applications*, vol. 1, 1994, pp. 69–78.

[22] M. C. Pérez, J. Ureña, A. Hernández, A. Jiménez, W. P. Marnane, and F. J. Álvarez, "Efficient real-time correlator for LS sequences," in *Proceedings of IEEE International Symposium on Industrial Electronics*, 2007, pp. 1663–1668.

[23] B. D. O. Anderson and J. B. Moore, *Optimal filtering*. Prentice-Hall, Englewood Cliffs, N. J., 1979, ch. 8, pp. 193–196.

[24] D. Gualda, J. Ureña, J. C. García, and A. Lindo, "Localization and Navigation using Locally Referenced Ultrasonic - LPS," *Sensors*, vol. 14, pp. 21 750–21 769, 2014.